Contribution from the Department of Inorganic Chemistry,
The Royal Institute of Technology, S-100 44 Stockholm, Sweden

Thermochromism in Copper(II) Complexes. Structures of the Red and Blue-Violet Forms of Bis(*N*,*N*-diethylethylenediamine)copper(II) Perchlorate and the Nonthermochromic Violet Bis(*N*-ethylethylenediamine)copper(II) Perchlorate

I. GRENTHE,*[1] P. PAOLETTI, M. SANDSTRÖM, and S. GLIKBERG[2]

Received March 9, 1979

The crystal and molecular structures of the title compounds have been determined by three-dimensional X-ray diffraction data by using an automatic four-circle diffractometer. The red low-temperature form of the thermochromic compound, studied at 25 °C, is triclinic, $P\bar{1}$, $Z = 1$, $a = 8.131$ (8) Å, $b = 8.762$ (13) Å, $c = 9.786$ (12) Å, $\alpha = 65.33$ (16)°, $\beta = 65.98$ (11)°, and $\gamma = 63.34$ (8)°, and the blue-violet high-temperature form studied at 60 °C is monoclinic, $I2$, $Z = 4$, $a = 13.34$ (1) Å, $b = 8.414$ (5) Å, $c = 9.978$ (5) Å, and $\beta = 97.43$ (5)°. The violet nonthermochromic compound, studied at 25 °C, is triclinic, $P\bar{1}$, $Z = 1$, $a = 8.131$ (8) Å, $b = 8.762$ (13) Å, $c = 9.786$ (12) Å, $\alpha = 65.33$ (16)°, $\beta = 65.98$ (11)°, and $\gamma = 63.34$ (8)°. The copper atom has a square-planar coordination geometry in both forms of the thermochromic compound but a tetragonally elongated octahedral coordination in the bis(*N*-ethylethylenediamine)copper(II) complex with weakly coordinated perchlorate oxygen atoms at the axial positions. The thermochromic behavior in bis(*N*,*N*-diethylethylenediamine)copper(II) perchlorate is thus not caused by a change in the axial coordination of copper(II) but is rather an effect of a change in the in-plane field strength. Although there is no significant difference in the Cu–N distance, the conformation of the ligands is different in the red and blue-violet forms of the thermochromic compound. In the high-temperature form a thermally induced inversion of the conformation of the copper–ethylenediamine rings seems to be the cause of large atomic movements perpendicular to the ring system. The ring inversion also results in large atomic motions of the ethyl side chains. This interpretation is supported by a proton magnetic resonance study, which indicates an averaging of the local magnetic fields by atomic motion. In the three compounds investigated the Cu–N bond distances increase significantly with increasing substitution on the amino group. A comparison with previously reported distances shows the weak axial interactions to have only a negligible influence on the Cu–N_4 in-plane bond lengths.

Introduction

Thermochromism is a well-known phenomenon in coordination chemistry and is usually ascribed to temperature-dependent changes in the coordination geometry of the chromophore. Thermochromic behavior in copper(II) complexes with N,N-substituted ethylenediamines has been discussed in some detail by Paoletti et al.[3,4] These authors try to explain the phenomenon in terms of geometrical factors such as changes in coordination numbers and coordination geometry. The discussion is to some extent impaired by the lack of direct structural information about the complexes.

Lever et al.[5,6] have suggested a temperature-dependent tetragonal distortion of the copper(II) coordination with an accompanying change in the d-orbital energies (cf. Figure 1) as a probable mechanism for thermochromism. The effect should then be similar to the well-known solvent effects on the spectra of copper(II) complexes.[7]

It is obvious that a quantitative test of some of the above proposals can be made by X-ray structure determinations of thermochromic complexes. In this communication, we will describe the structures of the red and blue-violet forms of the thermochromic bis(*N*,*N*-diethylethylenediamine)copper(II) perchlorate. For comparison, the violet nonthermochromic bis(*N*-ethylethylenediamine)copper(II) perchlorate is also described. This compound was selected in order to study the importance of steric interference from the side chains on the axial coordination. The compounds are denoted I-red, I-blue, and II, respectively. The structure of I-red was published by Curet et al.[11] before this study was completed.

Experimental Section

Preparation of Complexes. I-red was prepared as described by Pfeiffer and Glaser.[12] It was recrystallized from water. The composition was checked by elemental analysis. I-blue was obtained by heating a mounted crystal of I-red above the transition temperature by passing a stream of heated air through the low-temperature device of the diffractometer. II was prepared analogously with I-red and purified by recrystallization from water. The purity was checked by elemental analysis.

X-ray Data Collection. The intensity data were collected at 25 ± 2 °C for I-red and II and at 60 ± 5 °C for I-blue, respectively, by using an automatic Syntex $P2_1$ four-circle diffractometer. The space groups were determined by axial photographs and the monoclinic symmetry for I-blue was checked by measurements of equivalent reflections. The unit cell parameters were refined by least-squares methods using high-angle reflections obtained with the diffractometer. Unit cell dimensions and details of the data collection are given in Table I.

In order to check the stability of the crystal and the diffractometer, we measured three check reflections at regular intervals during the data collection; cf. Table I. The method for background measurement and intensity calculation has been described elsewhere.[13] Intensity data for ten selected reflections, with 2θ values evenly distributed over the 2θ range investigated, were measured for a full 360° rotation around the diffraction vector. These data were used to correct the intensities in the appropriate 2θ intervals for absorption. This semiempirical absorption correction method is described in ref 14.

Structure Determination and Refinement. The copper atom was located at the origin in all structures. The positions of chlorine were obtained from Patterson maps and the positions of the remaining nonhydrogen atoms from a subsequent difference electron density map. The hydrogen atoms were located in a new difference map calculated by using the least-squares refined positional and isotropic thermal parameters of the nonhydrogen atoms. No hydrogen atom positions could be located in I-blue.

The atom parameters for I-red, I-blue, and II are given in Tables II–IV. Details of the refinements are given in Table I. Some distances and angles of interest for the following discussion are given in Table V. Tables of $|F_o|$ and F_c and thermal parameters are available.[15]

NMR Measurements. Proton NMR spectra of the thermochromic compound were recorded on a Bruker CXP 100 instrument using the Fourier transform technique. The sample was studied in the temperature range 0–72 °C by using a 10-mm stationary NMR tube. The temperature was measured with a thermocouple. The line widths at the various temperatures are given in Table VI.

Structure Description and Discussion

I-Red. The positional and thermal parameters are in good agreement with those previously reported[11] after transformation from $P\bar{1}$ to $C\bar{1}$. The transformation matrix is 0, 1, 0; $-{}^1/_2$, ${}^1/_2$, 0; $-{}^1/_2$, ${}^1/_2$, -1. The latter space group was used by Curet et al.[11] The only difference between the two structure determinations was the location of two hydrogen atoms, H9 and H11, located on a methyl group in one of the side chains. The parameters reported here are in better agreement with the ideal geometry of a methyl group than those reported by

0020-1669/79/1318-2687$01.00/0

Table I. Crystal Data and Details of Data Collection and Refinement

	I-red	I-blue	II
	Crystal Data		
mol formula	$[Cu(Et_2NCH_2CH_2NH_2)_2](ClO_4)_2$	=I-red	$[Cu(EtNHCH_2CH_2NH_2)_2](ClO_4)_2$
space group	$P\bar{1}$ (triclinic)	$I2$ (monoclinic)	$P\bar{1}$ (triclinic)
unit cell parameters[a]	$a = 8.131\ (8)$ Å, $\alpha = 65.33\ (16)°$ $b = 8.762\ (13)$ Å, $\beta = 65.98\ (11)°$ $c = 9.786\ (12)$ Å, $\gamma = 63.34\ (8)°$	$a = 13.34\ (1)$ Å $b = 8.414\ (5)$ Å, $\beta = 97.43\ (5)°$ $c = 9.978\ (5)$ Å	$a = 7.595\ (3)$ Å, $\alpha = 73.86\ (3)°$ $b = 7.798\ (4)$ Å, $\beta = 70.85\ (2)°$ $c = 8.736\ (3)$ Å, $\gamma = 64.16\ (2)°$
radiation used	graphite-monochromatized Mo Kα, λ 0.71069 Å	graphite-monochromatized Mo Kα, λ 0.71069 Å	graphite-monochromatized Mo Kα, λ 0.71069 Å
V (Å^3), Z, D_x (g/cm^3), $\mu_{\mathrm{Mo\,K}\alpha}$ (cm^{-1})	545 (1), 1, 1.51, 13.3	1110 (1), 4, 1.48, 13.1	434.3 (3), 1, 1.68, 16.6
scan technique and part of reflctn sphere investigated	ω–2θ scan, $2\theta < 50°$	ω–2θ scan, $2\theta < 50°$	ω–2θ scan, $2\theta < 50°$
max and min scan speed	29.3 and 1.0 deg/min	29.3 and 1.0 deg/min	29.3 and 2.0 deg/min
no. of reflctns measd	1892	1306	1659
no. of reflctns obsd[b]	1755	846	1464
check reflctns measd	3 after every 50th reflctn, constant within ±5%	3 after every 30th reflctn, constant within ±25%	3 after every 50th reflctn, constant within ±2%
largest remaining peak in final difference Fourier	0.46 e Å^{-3}	0.35 e Å^{-3}	0.4 e Å^{-3}
	Data Reduction and Refinement		
type of absn correctn	semiempirical		semiempirical
max correctn	24%		22%
scattering factors	for neutral atoms; Cu and Cl with anomalous dispersion corrections		
no. of parameters refined in final model	188	122	142
least-squares refinemts[c] with non-H atoms anisotropic: $R(R_w)$[13]	0.041 (0.059)	0.074 (0.089)	0.030 (0.042)
largest parameter shift in the last refinemt cycle	$<0.06\sigma$	$<0.4\sigma$	$<0.01\sigma$
const C in wt function w[c]	0.03	0.04	0.03
std dev of observn of unit wt S	1.74	1.87	1.18

[a] The unit cell parameters for I-blue are after transformation from $I2$ to $P\bar{1}$ $a = 8.40\ (1)$ Å, $b = 8.85\ (2)$ Å, $c = 9.77\ (1)$ Å, $\alpha = 64.5\ (1)°$, $\beta = 64.5\ (1)°$, $\gamma = 61.7\ (1)°$, and $V = 555\ (1)$ Å^3. [b] Reflections with $|F_o| < 3.92\sigma(F_o)$ are given zero weight. [c] Function minimized: $\Sigma_i w_i(|F_o| - |F_c|)^2$ where $w_i = [\sigma_{\mathrm{count}}^2 + C|F_o|^2]^{-1}$.

Table II. Compound I-red Final Fractional Atomic Positional Parameters[a]

atom	x	y	z
Cu	0	0	0
Cl	0.2444 (1)	0.2807 (1)	0.1608 (1)
N1	0.1338 (5)	−0.2284 (4)	−0.0581 (3)
N2	−0.0663 (4)	−0.1205 (3)	0.2383 (3)
C1	0.2416 (5)	−0.1955 (5)	−0.2239 (4)
C2	0.1243 (5)	−0.0200 (5)	−0.3125 (4)
C3	−0.2309 (6)	−0.1742 (6)	0.2628 (4)
C4	−0.3318 (8)	−0.2506 (8)	0.4289 (6)
C5	−0.0881 (5)	0.2792 (5)	−0.3002 (4)
C6	−0.2769 (6)	0.2501 (6)	−0.2409 (8)
O1	0.3584 (4)	0.3906 (4)	0.1074 (5)
O2	0.2547 (7)	0.2232 (8)	0.0434 (5)
O3	0.3098 (7)	0.1282 (5)	0.2789 (5)
O4	0.0527 (5)	0.3732 (7)	0.2244 (8)
H1	0.217 (6)	−0.304 (5)	0.003 (5)
H2	0.053 (10)	−0.253 (10)	−0.057 (9)
H3	0.268 (5)	−0.286 (5)	−0.266 (4)
H4	0.359 (6)	−0.197 (5)	−0.227 (4)
H5	0.195 (7)	0.007 (6)	−0.404 (6)
H6	−0.001 (5)	0.041 (5)	0.301 (4)
H7	−0.319 (5)	−0.075 (5)	0.212 (4)
H8	−0.176 (6)	−0.262 (6)	0.219 (5)
H9	0.355 (13)	0.183 (13)	0.481 (11)
H10	−0.442 (9)	−0.250 (8)	0.442 (7)
H11	0.242 (10)	0.365 (10)	0.525 (9)
H12	0.095 (5)	−0.372 (5)	0.266 (4)
H13	0.026 (6)	−0.315 (7)	0.426 (6)
H14	0.294 (10)	−0.187 (10)	0.296 (9)
H15	0.381 (11)	−0.360 (11)	0.318 (9)
H16	0.314 (7)	−0.210 (7)	0.133 (7)

[a] Estimated standard deviations in parentheses.

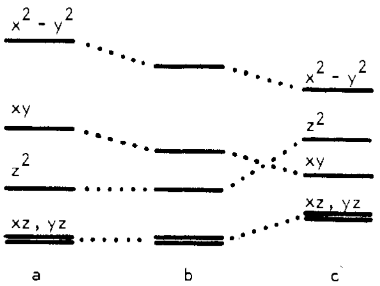

Figure 1. Schematic one-electron orbital energy level diagram of copper(II) in en complexes of D_{4h} symmetry, constructed from information in ref 7–10: (a) square-planar symmetry (Cu–N$_4$), (b) square planar with decreasing in-plane bond strength, (c) tetragonally distorted octahedral symmetry with weak axial interactions.

Table III. Compound I-blue Final Fractional Atomic Positional Parameters[a]

atom	x	y	z
Cu	0	0	0
Cl	0.2178 (2)	−0.4974 (5)	0.0584 (2)
N1	0.1458 (7)	−0.0042 (22)	0.0843 (7)
N2	0.0653 (6)	0.0113 (17)	−0.1749 (7)
C1	0.2177 (10)	−0.0053 (26)	−0.0109 (11)
C2	0.1706 (9)	0.0005 (37)	−0.1412 (11)
C3	0.0163 (13)	0.0822 (40)	−0.2958 (12)
C4	0.0088 (11)	0.2391 (23)	−0.2379 (17)
C5	0.0248 (29)	−0.1751 (31)	−0.2127 (23)
C6	0.0421 (23)	−0.2681 (22)	−0.3154 (26)
O1	0.2646 (10)	−0.6324 (16)	0.1130 (13)
O2	0.1246 (12)	−0.5464 (28)	0.0083 (19)
O3	0.2545 (17)	−0.4320 (25)	−0.0386 (16)
O4	0.2148 (22)	−0.3999 (18)	0.1502 (14)

[a] Estimated standard deviations in parentheses. The equivalent positions in the nonstandard setting $I2$ of space group No. 5 are $\bar{x}, y, \bar{z}$; $^1/_2 + x$, $^1/_2 + y$, $^1/_2 + z$; and $^1/_2 - x$, $^1/_2 + y$, $^1/_2 - z$.

Curet et al.[11] The reader is referred to these authors for a general description of the crystal and molecular structure of the compound. Figures 2 and 3 show the complex and the unit

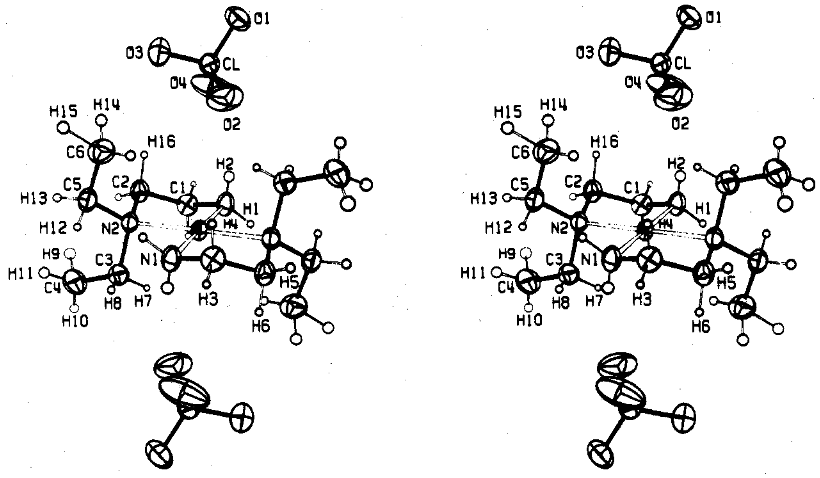

Figure 2. I-red. A stereoscopic view of the centrosymmetric bis(*N*,*N*-diethylethylenediamine)copper(II) complex ion and of the perchlorate ions closest to copper. The square-planar copper–nitrogen interactions are shown by the unfilled bonds. The thermal ellipsoids are drawn to include 30% probability. For clarity the isotropic H atoms are shown on the 10% level.

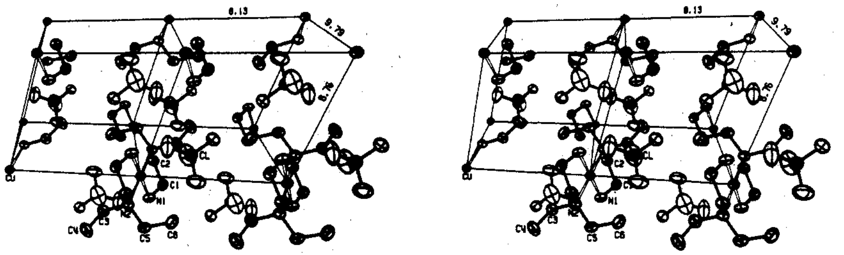

Figure 3. I-red. A stereoscopic view showing the molecular packing. The cell edges of two unit cells are outlined. The H atoms are omitted.

Table IV. Compound II Final Fractional Atomic Positional Parameters[a]

atom	*x*	*y*	*z*
Cu	0	0	0
Cl	0.2292 (1)	0.2714 (1)	0.1216 (1)
N1	0.2350 (4)	0.8278 (4)	0.8504 (3)
N2	0.0304 (4)	0.8007 (4)	0.2065 (3)
C1	−0.2368 (5)	0.0797 (5)	0.3205 (4)
C2	−0.1648 (5)	0.8654 (5)	0.3286 (4)
C3	0.2101 (6)	0.7601 (5)	0.2632 (5)
C4	0.2635 (9)	0.5818 (6)	0.3919 (6)
O1	0.3362 (4)	0.1417 (4)	0.2433 (3)
O2	0.2257 (4)	0.1633 (4)	0.0156 (3)
O3	0.3298 (4)	0.3996 (4)	0.0311 (3)
O4	0.0273 (4)	0.3820 (4)	0.1990 (4)
H1	0.232 (6)	0.728 (6)	0.866 (5)
H2	0.348 (5)	0.808 (4)	0.875 (4)
H3	−0.367 (5)	0.131 (4)	0.394 (4)
H4	−0.147 (5)	0.112 (5)	0.353 (4)
H5	−0.144 (5)	0.809 (5)	0.428 (4)
H6	0.726 (6)	0.850 (6)	0.312 (5)
H7	0.051 (6)	0.713 (5)	0.182 (5)
H8	0.323 (6)	0.721 (6)	0.169 (5)
H9	0.174 (6)	0.859 (6)	0.313 (5)
H10	0.157 (9)	0.588 (8)	0.496 (9)
H11	0.394 (7)	0.570 (6)	0.392 (6)
H12	0.290 (8)	0.457 (8)	0.346 (6)

[a] Estimated standard deviations in parentheses.

cell of I-red. It is obvious that the steric interference with the ethyl side chains prevents coordination of the perchlorate group to the copper atom.

There are no strong hydrogen bonds in the structure and the side chains have fairly large average contact distances to adjacent atoms. The temperature factors of the atoms in the side chains are not unexpectedly large and there is no indication of any positional disorder.

Table V. Interatomic Distances (in Å) and Angles (deg)[a]

	I-red	I-blue	II
Cu–N1	2.001 (3)	2.016 (9)	2.013 (3)
Cu–N2	2.068 (2)	2.051 (7)	2.031 (3)
Cu–O2	3.65 (1)	4.16 (2)	2.594 (3)
N1–C1	1.471 (5)	1.43 (2)	1.465 (4)
N2–C2	1.487 (5)	1.40 (2)	1.483 (5)
N2–C3	1.510 (6)	1.43 (2)	1.480 (6)
N2–C5	1.492 (5)	1.69 (3)	
C1–C2	1.507 (5)	1.37 (2)	1.503 (5)
C3–C4	1.504 (6)	1.45 (4)	1.517 (6)
C5–C6	1.504 (8)	1.33 (4)	
C1–O1	1.430 (4)	1.37 (2)	1.437 (3)
C1–O2	1.396 (6)	1.27 (2)	1.428 (3)
C1–O3	1.406 (6)	1.34 (2)	1.427 (3)
C1–O4	1.404 (6)	1.23 (2)	1.430 (3)
N1–Cu–N2	84.9 (1)	82.1 (5)	85.0 (1)
N1–Cu–N1	180	178.0 (5)	180
N2–Cu–N2	180	174.7 (4)	180
N1–Cu–O2	122.4 (1)	112.7 (5)	90.1 (1)
N2–Cu–O2	90.4 (1)	98.8 (4)	81.6 (1)

[a] Estimated standard deviations in parentheses.

Table VI. Half-Widths, d_1 and d_2 (in ppm), of the Two Lines in the Proton Magnetic Resonance Spectra of the Thermochromic Compound I

temp/°C	color	d_1	$10^{-1}d_2$
0	red	22	39
27	red	20	42
31	red	20	35
54	blue-violet	16	24
58	blue-violet	16	25
67	blue-violet	15	24
72	blue-violet	14	26

I-Blue. In the high-temperature form the copper(II) complex has a different conformation from that in I-red (cf. Figures 2 and 4). The space group symmetry requires a twofold rotational symmetry perpendicular to the Cu(en)$_2$ (en = ethylenediamine) ring system in I-blue, while there is a center of symmetry (at the Cu location) in I-red. There are

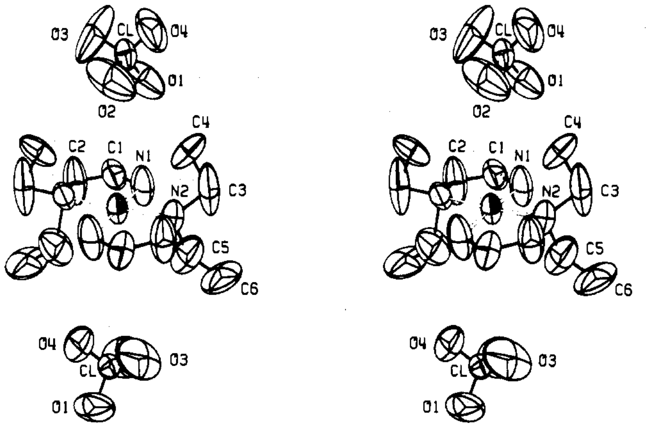

Figure 4. I-blue. A stereoscopic picture of the high-temperature modification with the thermal ellipsoids on the 30% probability level.

several noticeable facts in the Cu(en) rings in I-blue: The distance C1–C2 is much shorter than expected, 1.37 (2) Å vs. 1.50 Å (Table V). The $Cu(en)_2$ ring system appears to be approximately planar, the largest deviation from a least-squares plane through the Cu–4N square is 0.10 (2) Å for C1, while the corresponding deviations for C1 and C2 in I-red are –0.313 (3) and 0.356 (5) Å, respectively. These features in the geometry of I-blue are certainly artifacts caused by either dynamic or static disorder for which average atomic positions are obtained in the calculations. Similar, although less pronounced, effects have been observed for the Cu(en) rings in a $Cu(en)_2H_2O^{2+}$ ion in another crystal structure study.[16]

From Figure 4 it is obvious that the atoms of the $Cu(en)_2$ rings have large amplitudes perpendicular to the ring. From a flexible model of the molecule it can easily be shown that a ring inversion, principally a dynamic flipping of the carbon atoms across the Cu–N1–N2 plane, can cause a movement of the ring atoms and of the ethyl groups bonded to N2 which is consistent with the observed anisotropies. Such an atomic motion will also affect the accuracy of the Cu–N bond lengths given in Table V.[16]

The perchlorate group also shows large anisotropies and apparent shortenings of the bond lengths (Figure 4 and Table V), probably due to extensive librational movements. The large thermal movements of the ethyl groups also cause a further increase of the closest distance from Cu to the perchlorate group, Table V.

By diffraction methods one cannot decide whether the anisotropies obtained are a result of large thermal motions around the average positions or an average of a statistical distribution over different sites in the structure (or from any combination of these possibilities). For reasons discussed below there seems to be, in this case, a rather unrestricted dynamic disorder between different conformations of the molecule.

It is interesting to note that the *rate* of transition between the red and blue forms is virtually instantaneous and is probably determined by the rate of heat transfer in the crystal. There is no indication of any deterioration in the quality of the low-temperature form of the crystal, even after several thermal cycles. The absence of disorder in I-red implies that the energy barrier between the different conformations must be fairly low.

Compound II. The structure of II is shown in Figures 5 and 6. The coordination geometry of the organic ligands is very similar in I-red and II. However, in II the less bulky ligand makes it possible for the perchlorate group to be coordinated. The packing of the complexes is also very similar in I-red and II; cf. Figures 3 and 6. There are three possible hydrogen bond distances in the structure, all with oxygen as acceptor atom. The average hydrogen–oxygen distance is 2.50 (5) Å, indicating very weak interactions. For the closely related compounds I-red and II the Cu–N distance increases about 0.03 Å for each successive substitution of an ethyl group on the amine nitrogen (Table V).

In Table VII precisely determined copper–nitrogen bond lengths for a number of substituted $Cu(en)_2$ complexes are compiled. Also here the average distances are about 0.03–0.04 Å longer for a secondary amine than for a primary. For the rather few tertiary amines there does not seem to occur any further increase in the Cu–N bond distance. The weak axial interactions do not seem to increase the in-plane Cu–N bond lengths noticeably.

NMR Measurements. The solid-state NMR spectrum of I-red and I-blue consists of two overlapping peaks, one of which

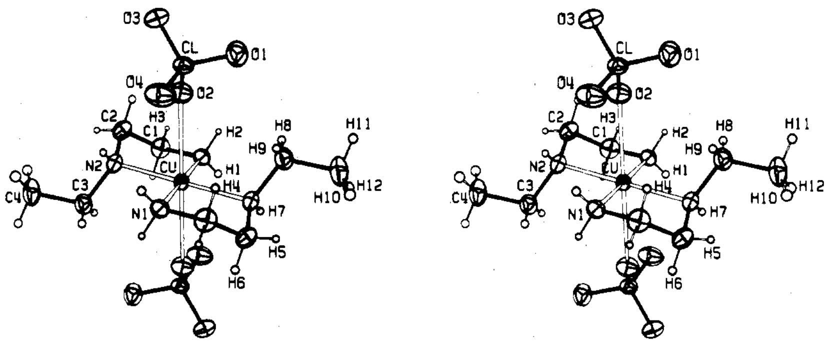

Figure 5. Compound II. A stereoscopic view of the molecular complex in bis(*N*-ethylethylenediamine)copper(II) perchlorate, shown in the same way as in Figure 2. The tetragonally distorted octahedral coordination around copper is shown by the unfilled bonds.

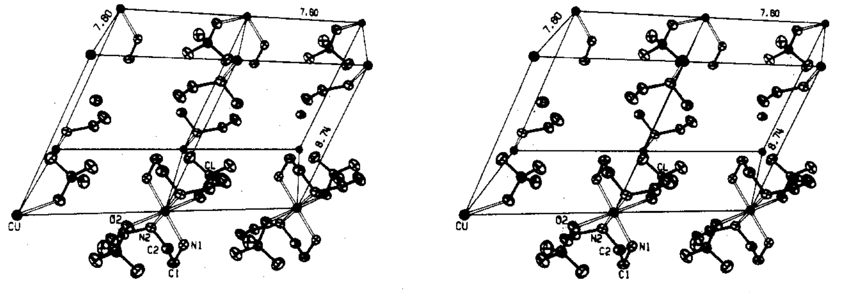

Figure 6. Compound II. A view of the molecular packing as in Figure 3.

Table VII. Survey of the Coordination around Copper in Various Bis(ethylenediamine)copper(II) Complexes[l]

compd	Cu–N (in plane)	Cu–X (axial)	abs max (color)	ref
$CuL_2(ClO_4)_2$[a]	p: 2 × 2.004 (5); s: 2 × 2.066 (5)	O: 2 × 2.575 (6)	18.8 (–)	17
$[CuL_2](ClO_4)_2$[b]	p: 2.012 (4), 2.018 (4); s: 2.036 (3), 2.041 (3)	O: 2.419 (3), 2.518 (3)	16.8 (dark blue)	18
$CuL_2(ClO_4)_2$[c] (=II)	p: 2 × 2.013 (3); s: 2 × 2.031 (3)	O: 2 × 2.594 (3)	(violet)	this work
$[CuL_2](ClO_4)_2$[d] (=I-red)	p: 2 × 2.001 (3); t: 2 × 2.068 (2)		20.6[k] (brick red)	this work
$[CuL_2](ClO_4)_2$[d] (=I-blue)	p: 2 × 2.016 (9); t: 2.051 (7)		19.7[k] (blue-violet)	this work
$Cu(en)_2(NCS)(ClO_4)$	p: 2 × 2.01 (1), 2 × 2.03 (1)	N: 2 × 2.73 (1)	18.5 (violet)	19
$CuL_2(NCS)_2$[e]	s: 2 × 2.062 (6), 2 × 2.064 (6)	N: 2 × 2.517 (7)	(green)	20
$CuL_2(SCN)_2$[a]	p: 2.029 (11), 2.049 (12); s: 2.067 (11), 2.070 (13)	N: 2.238 (14) S: 3.348 (4)	17.1 (violet)	21
$CuL_2(NO_3)_2$[a]	p: 2 × 2.01 (1); s: 2 × 2.05 (1)	O: 2 × 2.54 (1)	18.2 (dark blue)	17
$CuL_2(H_2O)_2(NO_3)_2$[f]	s: 2 × 2.055 (4), 2.082 (4)	H_2O: 2 × 2.489 (4)	17.4 (blue violet)	17
CuL_2Cl_2[b]	p: 2 × 2.018 (5); s: 2 × 2.059 (5)	Cl: 2.831 (2)	17.8 (blue)	21
$CuL_2(H_2O)_2{\cdot}C_2O_4$[a]	p: 2 × 2.008 (5), s: 2 × 2.057 (5)	H_2O: 2 × 2.503 (5)	18.2 (dark violet)	22
$CuL_2{\cdot}L'{\cdot}2H_2O$[a,g]	p: 2.014 (8), 2.019 (8); s: 2.040 (8), 2.054 (8)	H_2O: 2.439 (8) O: 2.630 (7)	17.7 (violet)	19
$Cu(en)_2(L')_2$[h]	p: 2 × 2.006 (2), 2 × 2.008 (2)	O: 2 × 2.517 (2)	(purple)	23
$CuL_2(L')_2$[i]	p: 2 × 1.989 (3), t: 2 × 2.064 (3)	O: 2 × 2.793 (2)	18.6 (purple)	24
$[CuL_2]L$[b,j]	p: 2 × 2.033 (4), s: 2 × 2.080 (4)	O: 2 × 2.510 (3)	(–)	25
$Cu_3(en)_2(CN)_4{\cdot}H_2O$	p: 2.004 (4), 2.004 (4), 2.017 (4), 2.034 (4)	O: 2.441 (4)	(pale purple)	16

[a] L = *N*-methylethylenediamine. [b] L = *N*-(2-hydroxoethyl)ethylenediamine. [c] L = *N*-ethylethylenediamine. [d] L = *N,N*-diethylethylenediamine. [e] L = *N,N'*-dimethylethylenediamine. [f] L = *N,N'*-diethylethylenediamine. [g] L' = *d*-tartrato. [h] L' = dodecyl sulfato. [i] L = *N,N*-dimethylethylenediamine, L' = 1,1,1,5,5,5,-hexafluoropentane-2,4-dionato. [j] L' = succinate. [k] From ref 6. [l] The bond lengths, uncorrected for thermal motion, are given in angstrom units and the estimated standard deviations within parentheses. The abbreviations are p = primary, s = secondary, and t = tertiary substituted amino group. The energy of the maximum absorption of the visible d–d band is given in $cm^{-1} \times 10^3$. The colors are cited from the original references.

is considerably broader than the other. The half-widths of the two peaks are given in Table VI. They occur at approximately the same position, which is shifted downfield about 8 ppm at the color change from red to blue-violet. For temperatures below and above this transition the line widths vary only slightly with temperature. However, there is a very noticeable line narrowing at the color change, especially of the broad peak in I-blue as compared to I-red. This line-width narrowing is consistent with an averaging of the local magnetic fields by large thermally induced atomic motions (rapid ring inversion) of the organic ligand in I-blue.

Mechanism of the Thermochromic Change. The maximum in the visible region of the electronic spectrum of bis(ethylenediamine)copper(II) compounds corresponds to the $d_{xz},d_{yz} \rightarrow d_{x^2-y^2}$ transition.[5–10] As pointed out by Lever et al.,[5,10] an increasing axial interaction will give a lower transition energy as the energies of the d_{xz}, d_{yz} and d_{z^2} orbitals rise (Figure 1). At the same time the $d_{x^2-y^2}$ and d_{xy} energies will decrease due to decreasing involvement of the Cu orbitals with the in-plane ligands. This mechanism is amply exemplified by the two modifications of bis(1,3-diaminobutane)copper(II) perchlorate with different colors and also with different axial interactions.[26] The perchlorate oxygen atom coordinated in the axial positions is 0.1 Å closer to copper in the blue-violet form than in the red-violet one.

However, in I-red and I-blue the steric interference of the ethyl groups is shown to prevent axial interactions with perchlorate oxygen atoms, thus explaining the unexpectedly large transition energies.[5,6] In these compounds the thermochromic behavior cannot be due to differences in axial interactions but rather to changes in the in-plane Cu–N bond energies by other causes.

On the other hand, the deep blue solution obtained upon dissolution of I-red implies a marked decrease of the transition energy.[5,4] This is certainly an effect of a coordination of solvent molecules in the axial positions.

The high-pressure studies by Ferraro et al.[4] indicate that the observed increase in the electronic transition energy corresponds to an increasing Cu–N in-plane field strength. On the other hand, the slow decrease of the energy of the main d–d band with increasing temperature, which is observed for I-red,[3,4] is consistent with decreasing strength of the Cu–N interactions. Moreover, from vibrational spectra, the blue forms of the thermochromic compounds have been found to have the lower force constants and therefore also the lower Cu–N bond strengths.[5] The expected change in the energy levels with decreasing in-plane field strength is qualitatively shown in Figure 1. Thus, the thermochromic change in this perchlorate compound, and certainly also in the closely related tetrafluoroborate, must be due to a sudden change of the in-plane field strength. Although no significant change is found in the Cu–N bond lengths, the ligand conformation is different and large thermally induced atomic movements occur in I-blue.

Acknowledgment. This work has been supported by grants from the Swedish Natural Science Research Council. The diffractometer is a generous gift from the Knut and Alice Wallenberg Foundation. The pleasant cooperation with Dr. Ulf Henriksson (for the NMR measurements) and Professor Oliver Lindqvist (for the loan of a Syntex diffractometer equipped with a high-temperature device) is gratefully acknowledged.

Registry No. I, 52646-62-5; II, 34195-59-0.

Supplementary Material Available: Listings of anisotropic thermal parameters and structure factor amplitudes for I-red, I-blue, and II (33 pages). Ordering information is given on any current masthead page.

References and Notes

(1) Author to whom correspondence should be addressed.
(2) Graduate Research Participant, 1977.
(3) L. Fabbrizzi, M. Micheloni, and P. Paoletti, *Inorg. Chem.*, **13**, 3019 (1974).
(4) J. R. Ferraro, L. J. Basile, L. R. Garcia-Ineguez, P. Paoletti, and L. Fabbrizzi, *Inorg. Chem.*, **15**, 2342 (1976); **16**, 2127 (1977).
(5) A. B. P. Lever, E. Mantovani, et al. *Inorg. Chem.*, **10**, 817, 2424 (1971).
(6) B. P. Kennedy and A. B. P. Lever, *J. Am. Chem. Soc.*, **95**, 6907 (1973).
(7) P. B. Heslop and K. Jones, "Inorganic Chemistry, A Guide to Advanced Study", Elsevier, Amsterdam, 1976, p 736.
(8) B. J. Hathaway, D. E. Billing, P. Nicholls, and I. M. Procter, *J. Chem. Soc. A*, 319 (1969).
(9) I. M. Procter, B. J. Hathaway, and P. Nicholls, *J. Chem. Soc. A*, 1678 (1968).
(10) A. B. P. Lever, "Inorganic Electronic Spectroscopy", Elsevier, Amsterdam, 1968, p 78.
(11) M. M. Andina, J. D. Curet, and M. M. Muir, *Acta Crystallogr., Sect. B*, **32**, 3185 (1976).
(12) P. Pfeiffer and H. Glaser, *J. Prakt. Chem.* **151**, 134 (1938).

(13) M. Sandström and I. Persson, *Acta Chem. Scand., Ser. A*, **32**, 95 (1978).

(14) G. Kopfmann and R. Huber, *Acta Crystallogr., Sect. A*, **24**, 348 (1968); A. C. T. North, D. C. Phillips, and F. Scott Mathews, *ibid.*, 351 (1968).

(15) Supplementary material.

(16) R. J. Williams, A. C. Larson, and D. T. Cromer, *Acta Crystallogr., Sect. B*, **28**, 858 (1972).

(17) E. Luukkonen, A. Pajunen, et al., *Suom. Kemistil. B*, **42**, 474, 348 (1969); **43**, 160 (1970).

(18) R. V. Chastain, Jr., and T. L. Dominick, *Inorg. Chem.*, **12**, 2621 (1973).

(19) M. Cannas, G. Carta, and G. Marongiu, *J. Chem. Soc., Dalton Trans.*, 251 (1973).

(20) J. Korvenranta and A. Pajunen, *Suom. Kemistil. B*, **43**, 119 (1970).

(21) R. Hämäläinen and A. Pajunen, *Suom. Kemistil. B*, **45**, 117, 122 (1972); *Finn. Chem. Lett.*, 150 (1974).

(22) R. Hämäläinen, *Suom. Kemistil. B*, **44**, 89 (1971); **46**, 237 (1973).

(23) P. J. M. W. L. Birker, P. T. Crisp, and C. J. Moore, *Acta Crystallogr., Sect. B*, **33**, 3194 (1977).

(24) M. A. Bush and D. E. Fenton, *J. Chem. Soc. A*, 2446 (1971).

(25) A. Pajunen, E. Näsäkkälä, and S. Pajunen, *Cryst. Struct. Commun.*, **7**, 63 (1978).

(26) A. Pajunen, K. Smolander, and I. Belinskij, *Suom. Kmistil. B*, **45**, 317 (1972).

Contribution from the Department of Chemistry,
University of Virginia, Charlottesville, Virginia 22901

High- and Low-Spin Interconversion in a Series of (α-Picolylamine)iron(II) Complexes

ANTHONY M. GREENAWAY, CHARLES J. O'CONNOR, ALAN SCHROCK, and EKK SINN*

Received March 27, 1979

The magnetic properties of $[Fe(\alpha\text{-}P)_3]Br_2\cdot S$ (α-P = α-picolylamine; S = methanol, ethanol) and $[Fe(\alpha\text{-}P)_3]Cl_2\cdot C_2H_5OH$ and the crystal structure of the latter complex have been determined. Each of the complexes is high spin at room temperature and each undergoes a similar transition to low spin in the region 130–90 K. In each case the transition is relatively sharp, being mostly complete in the region 130–110 K, and is sharper than in the analogous complex $[Fe(\alpha\text{-}P)_3]Cl_2\cdot CH_3OH$. We noted earlier that $[Fe(\alpha\text{-}P)_3]^{2+}$ has approximate threefold symmetry in the purely low-spin $[Fe(\alpha\text{-}P)_3]Cl_2\cdot 2H_2O$ (*fac* geometry) but has one of its ligands coordinated with the two donor atoms reversed in $[Fe(\alpha\text{-}P)_3]Cl_2\cdot CH_3OH$ (*mer* geometry). The crystal structure of $[Fe(\alpha\text{-}P)_3]Cl_2\cdot C_2H_5OH$ and the similarity of the magnetic properties indicate that the present complexes all have the same "ligand-reversed" structure of the $[Fe(\alpha\text{-}P)_3]^{2+}$ ion. Removal of the included solvent S drastically alters the magnetic properties, eliminating the sharp spin transition and replacing it with a spin equilibrium which is so gradual that low spin ($^1A_1$) is not attained even at the lowest temperatures studied (4 K). Literature observations of such very gradual spin transitions can now be explained in terms of sample drying which removed solvent that had originally been held in the lattice via hydrogen bonding. The crystal structure of $[Fe(\alpha\text{-}P)_3]Cl_2\cdot C_2H_5OH$ reveals hydrogen bonding between the ethanol molecule and a halogen but not with the cation. Comparison of this structure with that of $[Fe(\alpha\text{-}P)_3]Cl_2\cdot 2H_2O$ reveals a large change, 0.18 Å, in the average metal–ligand bond length between the high-spin and low-spin iron(II) species, providing important support for our previous determination of 0.19 Å for this quantity. Crystal data for $[Fe(\alpha\text{-}P)_3]Cl_2\cdot C_2H_5OH$: space group $P2_1/c$, $Z = 4$, $a = 10.937$ (5) Å, $b = 22.061$ (9) Å, $c = 11.571$ (6) Å, $\beta = 116.70$ (4)°, $V = 2496$ Å^3, $R = 5.3\%$ for 1470 reflections.

Introduction

Complexes lying near the high-spin–low-spin crossover have been shown to be very sensitive to changes in temperature and pressure, minor chemical changes in the ligands, counteranions in the case of cationic complexes, and solvent molecules incorporated in the lattice.[1-12] Quite dramatic solvent effects have been demonstrated in ferric dithiocarbamates,[5-8] in the iron(III) complexes of B_2trien (B = salicylaldehyde, acetylacetone, 3-chloroacetylacetone)[9,10] and in the iron(II) complexes $[Fe(\alpha\text{-}P)_3]Cl_2$ (α-P = α-picolylamine).[12] In the complexes $[Fe(B_2trien)]^+X^-$ (where X = Cl, NO_3), inclusion of water molecules, simultaneously hydrogen bonded to both the cation and the anion, induces a low-spin state, while analogous anhydrous complexes tend to be pure high spin or to exhibit a high-spin–low-spin equilibrium.[9,10] Similarly, the water molecules in the low-spin $[Fe(\alpha\text{-}P)_3]Cl_2\cdot 2H_2O$ (*fac* structure A, Figure 1) are hydrogen bonded to both the cations and the anions, while there is no link between the methanol and the cations in $[Fe(\alpha\text{-}P)_3]Cl_2\cdot CH_3OH$ (*mer* structure B, Figure 1), which exhibits a high-spin–low-spin equilibrium.[11] We show here that occluded solvent molecules in $[Fe(\alpha\text{-}P)_3]Cl_2\cdot C_2H_5OH$, which also exhibits the spin equilibrium, are likewise isolated from the cations. Whether the magnetic differences are induced directly by the solvent molecules or indirectly by inducing structural differences or both is now an important question. We present evidence which suggests that, while solvent–cation contact is important if only by reducing the amount of anion–cation contact, the cation structures A and B are magnetically different, the more distorted B tending to have the weaker crystal field (closer to high spin). Inclusion of hydrogen-bonding solvents, such as chloroform, dichloromethane, or water, in ferric dithiocarbamate lattices tends to shift the spin-state equilibrium toward the high-spin side and to lower the energy of the intermediate $S = {}^3/_2$ spin state.[5-8] Similarly, the high residual magnetic moment at low temperatures reported[13] for $[Fe(\alpha\text{-}P)_3]Br_2$ but not for $[Fe(\alpha\text{-}P)_3]Cl_2$ raises the question of a low-lying intermediate spin state ($S = 1$) for the bromide complex. We show here that no low-lying intermediate spin state exists in $[Fe(\alpha\text{-}P)_3]Br_2\cdot S$ (S = CH_3OH, C_2H_5OH), but that a spin-state crossover involving $S = 0$ ($^1A_1$) and $S = 2$ ($^5T_2$) states exists in each of the complexes $[Fe(\alpha\text{-}P)_3]X_2\cdot S$ (X = Cl, Br; S = CH_3OH, C_2H_5OH). A magnetic study of an ethanol solvated complex, after desolvating, raises new questions however.

Experimental Section

The complexes were prepared as described[14,15] by Sorai et al. The syntheses were carried out by using Schlenk apparatus, and the recrystallizations and all product handling were carried out in a dry nitrogen atmosphere. The desolvated complex $[Fe(\alpha\text{-}P)_3]Br_2$ was prepared by pumping the ethanol solvated complex $[Fe(\alpha\text{-}P)_3]Br_2\cdot C_2H_5OH$ on a high-vacuum line at 80 °C for 24 h. Magnetic susceptibilities and moments were determined by using a superconducting susceptometer incorporating a Josephson junction magnetometer, superconducting magnets, and shields.[7]

Crystal data for $[Fe(\alpha\text{-}P)_3]Cl_2\cdot C_2H_5OH$: $FeCl_2O_2N_6C_{20}H_{30}$; mol wt 493; space group $P2_1/c$; $Z = 4$; $a = 10.937$ (5), $b = 22.061$ (9), $c = 11.571$ (6) Å; $\beta = 116.70$ (4)°; $V = 2496$ Å^3; $\rho_{calcd} = 1.31$, $\rho_{obsd} = 1.30$ g cm^{-3}; μ(Mo Kα) = 8.6 cm^{-1}; crystal dimensions (in mm from centroid) (100) 0.05, ($\bar{1}00$) 0.05, (010) 0.15, ($0\bar{1}0$) 0.15, (001) 0.15, (001) 0.15; maximum and minimum transmission coefficients = 0.95, 0.92.

The crystal was mounted in a glass capillary in a nitrogen atmosphere to protect it from oxygen and water. The Enraf-Nonius program SEARCH was used to obtain 25 accurately centered reflections which were then used in the program INDEX to obtain approximate